Observation of a 111.9 nm Narrow Spectral Line Emitted from Ne-Like Al Ion in Laser-Produced Plasmas

Yu TAKEHIRO[1)], Shusen GAO[1)], Yuito NISHII[1)],
Maki KISHIMOTO[1)], Tomoyuki JOHZAKI[1,2)], Kotaro YAMASAKI[1)],
Takeshi HIGASHIGUCHI[3)], Shinichi NAMBA[1)]*

[1)] *Graduate School of Advanced Science and Engineering, Hiroshima University, Hiroshima 739-8527, Japan*
[2)] *Institute of Laser Engineering, Osaka University, Osaka 565-0871, Japan*
[3)] *Department of Electrical and Electronic Engineering, Utsunomiya University, Tochigi 321-8505, Japan*

(Received 29 August 2025 / Accepted 21 October 2025)

Short-wavelength lasers based on a transient collisional excitation (TCE) have extensively been studied using neon (Ne)-like and nickel (Ni)-like ions. In this study, we have examined the possibility of amplified spontaneous emission (ASE) at 111.9 nm in a Ne-like aluminum (Al) plasma using the TCE scheme. Al targets in vacuum were irradiated with two time-delayed Nd:YAG laser pulses (wavelength: 1,064 nm). A pre-pulse laser generated a pre-formed plasma, and subsequently a grazing-incidence main-pulse laser axially heated it to excite $3p$ ($1S^0$)–$3s$ ($1P^1$) transition of Al^{3+} ion. To achieve effective energy deposition in the region of electron density of $\sim 10^{18}$ cm^{-3}, the main-pulse was introduced at 3.5° incidence angle. Under optimized conditions, a sharp spectral line at 111.9 nm, corresponding to the $3p$–$3s$ lasing transition in Ne-like Al ion, was observed. Although clear ASE was not observed, this work confirms the feasibility of vacuum ultraviolet (VUV) ASE generation by means of this scheme. Further improvements in pulse synchronization and irradiation conditions would show the prominent evidence of 111.9-nm ASE phenomenon.

Keywords: laser produced aluminum plasma, VUV laser, transient collisional excitation scheme

DOI: 10.1585/pfr.21.2401004

1. Introduction

Since the invention of the laser in the 1960s, laser technologies have been extensively developed for a wide range of applications [1]. Short-wavelength lasers in the extreme ultraviolet (EUV) and soft x-ray regions have attracted significant attention due to their applications, such as biomedical imaging [2]. In the vacuum ultraviolet (VUV) region, high-power argon excimer lasers at 126 nm have already been demonstrated [3]. However, excimer lasers generally exhibit a broad spectral bandwidth, which limits their application in high-resolution spectroscopy and interferometry. Therefore, there is still a strong demand for narrow-band coherent light sources based on atomic transitions, such as the $3p$–$3s$ transition of Ne-like Al ions. Among various approaches to generating population inversion in highly ionized plasmas, a transient collisional excitation (TCE) scheme has proven to be one of the most effective methods for achieving laser oscillation at short wavelengths [1, 4].

*Corresponding author's e-mail: namba@hiroshima-u.ac.jp

This article is based on the presentation at the Joint Conference of the 22nd International Conference on Atomic Processes in Plasmas (APiP 2025) and 1st NIFS Conference on Atomic and Molecular Processes in Plasmas.

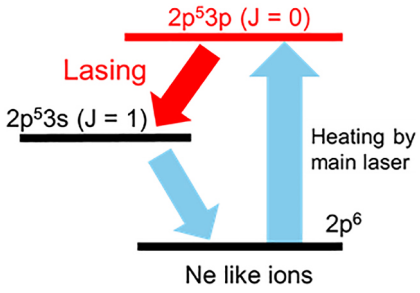

Fig. 1. Partial energy level diagram of Ne-like Al ion.

In the TCE scheme, two pulse lasers are used for generation of plasma and subsequent excitation. Firstly, Ne-like Al ions in the ground state ($2p^6$) are generated by a nanosecond pre-pulse laser. Secondly, by irradiation of a short main-pulse, collisional excitation between $2p$ and $3p$ levels occurs dominantly, resulting in population inversion between $3p$ and $3s$ of Al^{3+} ions, as shown in Fig. 1.

To date, the TCE x-ray lasers have been demonstrated using Ne-like and Ni-like ions, producing spatially coherent emissions with wavelengths ranging from 7.3 nm (samarium) to 87.6 nm (silicon) [5, 6]. These results have expanded the frontier of intense short-wavelength light sources. However, there remains a wavelength gap between conventional

ultraviolet (UV) lasers, such as, F_2 laser (157 nm) and soft x-ray lasers (46.9 nm, Ne-like Ar laser) [7], which limits the development of certain applications in the VUV region.

In this context, aluminum plasmas have emerged as a promising candidate for VUV laser oscillation. According to atomic structure calculations, Ne-like Al ion exhibits a $3s$–$3p$ transition at approximately 111.9 nm [8]. If an amplified spontaneous emission (ASE) could be achieved at this wavelength using the TCE scheme, it would represent the longest wavelength demonstrated, effectively bridging the gap between UV and soft x-ray lasers.

2. Principle

To optimize plasma parameters, the Saha equation and scaling law were examined as a first approximation. The Saha equation showed that the electron temperature at which Al^{3+} became dominant ionic species was approximately 3 eV. However, it should be noted that the Saha equation assumes thermal equilibrium, while actual laser-produced plasmas are in non-local thermal equilibrium (LTE) conditions where electron and ion temperatures are not the same. Considering non-LTE effects, the parameters for lasing action are expected to be narrower than those obtained here, but it is sufficient for rough estimation for the plasma parameters.

For Ne-like ions from silicon (Si) to selenium (Se), the scaling law was proposed and described how the gain coefficient, G, and other physical quantities vary depending on the plasma properties of Ne-like ions [9, 10]. The scaling law is given by,

$$G = 1.1 \times 10^{-16} f_{12} \lambda_{21} \frac{g_1}{g_2} \left(\frac{3\mu}{T_e}\right)^{\frac{1}{2}} N_2 \left(1 - \frac{g_2 N_1}{g_1 N_2}\right), \quad (1)$$

$$\Delta E_{02} = 2.25 (Z - 6.4)^{1.94}, \quad (2)$$

$$\lambda_{21} = 2867 (Z - 10.1)^{-0.87}, \quad (3)$$

where f_{12} is the oscillator strength, λ_{21} is the lasing wavelength (nm), g is the statistic weights of the corresponding levels, μ is the ion mass in atomic units, T_e is the excitation temperature, ΔE_{02} is the egergy separation (eV) between the ground state ($2p$) and the upper lasing level ($3p$) of the Ne-like ion, Z is the atomic number. Here, the excitation temperature corresponds to the electron temperature rapidly heated by the main laser with a pulse duration of a few ps or less. Since the scaling law can be considered a very good approximation for low atomic number elements, it may be applied to Al ion, whose atomic number is one less than that of Si. The gain coefficient for Ne-like Al laser for various excitation temperature is shown in Fig. 2. The gain coefficient exceeds 10 for the pre-plasma with electron density of 3×10^{18} cm^{-3} and the excitation temperature of 263 eV, as indicated by the star symbol in Fig. 2. Therefore, the generation of low temperature (3 eV) and low density (3×10^{18} cm^{-3}) plasma and subsequent plasma heating are essential for creating the population inversion.

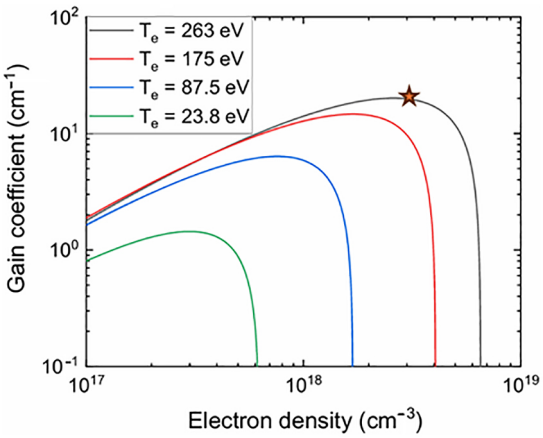

Fig. 2. Calculated gain coefficient of the Ne-like Al laser for various excitation temperatures.

The optimal electron density of pre-plasma is found to be 3×10^{18} cm^{-3}, whereas the critical density, n_{cr}, for Nd:YAG laser (λ = 1,064 nm) is 10^{21} cm^{-3}. In order to compensate for the difference in these electron densities, the GRIP (GRazing Incidence Pumping) scheme was applied in this study [11]. The GRIP scheme reduces the effective electron density by irradiating the laser beam at an oblique incidence instead of normal incidence angle. The effective electron density, $n_{cr\,effective}$, is given by the following equation,

$$n_{cr\,effective} = n_{cr} \cos^2(90 - \theta), \quad (4)$$

where θ is an incident angle of the laser with respect to the target surface. From Eq. (4), for the incident angle of 3.5° the effective electron density becomes approximately 3×10^{18} cm^{-3} which is equivalent to the optimal electron density for the Ne-like Al ion laser.

To generate plasmas having these plasma parameters, the intensity and irradiation timing of the two lasers must be adjusted properly. Therefore, the characteristics of Al plasmas produced by the pre-pulse laser were examined using a two-dimensional radiation hydrodynamic code, Star2D [12], which is based on a one-fluid, two-temperature radiation hydrodynamics model.

Because nanosecond-scale calculations require significant computational resources, Star2D first treats the early expansion phase in the x-direction with a one-dimensional Lagrangian method, where the computational grid follows the fluid motion. Since the laser has an intensity distribution along the y-direction, the x-direction motion is calculated for each y-point of the Eulerian grid, and the initial two-dimensional distribution is reconstructed by superimposing these results. The Lagrangian approach is applied until the plasma with subcritical density has expanded sufficiently, ensuring adequate mesh resolution upon remapping to the Eulerian grid. In this stage, the surrounding gas is neglected. The calculation is then remapped onto the Eulerian grid, surrounding gas is introduced, and the subsequent evolution is computed using the Eulerian method.

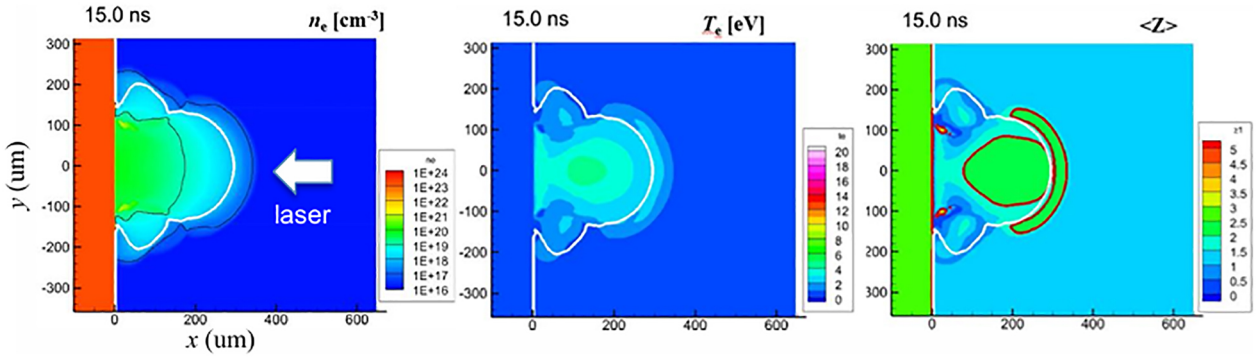

Fig. 3. Two-dimensional cross-sectional distribution of plasma parameters at 15 ns after pre-pulse irradiation, calculated using the Star2D code. (a) electron density, (b) electron temperature, and (c) average ion charge state. The vertical axis corresponds to the normal distance from the target surface, and the horizontal axis represents the lateral distance across the elongated plasma column.

The simulation conditions are as follows: The laser wavelength: 1,064 nm, pulse duration: 7.6 ns, peak intensity of pre-pulse: 1.0×10^9 W cm^{-2}, line-focal width: 150 μm (y-direction, full-width at half maximum: FWHM), $x = 0$ μm: target surface. The lasing medium is generated along z-axis, so that the cross section of the plasma in the z plane is calculated. In this simulation, the plasma column generated by the line-focused pre-pulse is assumed to be homogeneous along the z-direction. Therefore, the edge effect that may influence the lasing action is not considered in this study. The simulation shows that the plasma at 15 ns after plasma generation when the laser was incident and had passed its peak intensity and this time corresponds to 5 ns after the peak time, as presented in Fig. 3. Figure 3(a) shows the electron density distribution, and the region around the white line corresponds to an electron density of 10^{18} cm^{-3}. Figure 3(b) plots the electron temperature distribution. The electron temperature around white line (10^{18} cm^{-3}) is approximately 3 eV. The distribution of the averaged ion charge states is shown in Fig. 3(c). The region enclosed by the red line indicates where Al^{3+} ions are dominant species, while again the white line represents the electron density of 10^{18} cm^{-3}. From Fig. 3, it can be confirmed that the region where Al^{3+} ions are dominant overlaps with the region where the electron density reaches 10^{18} cm^{-3}. The overlap of these regions is an essential condition for the pre plasma, and subsequent creation of the population inversion. Therefore, the main pulse was set to be irradiated within 15 ns after the pre-pulse was incident on the target.

3. Experimental Set Up

Figure 4 shows a schematic diagram of the experimental set up to measure VUV emission from laser produced Al plasmas. In this study, a nanosecond Nd:YAG laser (Continuum Powerlite, 1,064 nm, 7.6 ns) was used as pre-pulse laser and line-focused onto the Al slab target. The line focal width and length were 150 μm and 12 mm, respectively, and the laser intensity was estimated to be 2.5×10^8 W cm^{-2}. A picosecond Nd:YAG laser (Continuum, custom laser, 1,064 nm, 12 ps) was used as the main-pulse laser of the GRIP scheme. The spot size (FWHM) on the pre-plasma was 100 μm and laser intensity was 4.2×10^{13} W cm^{-2}.

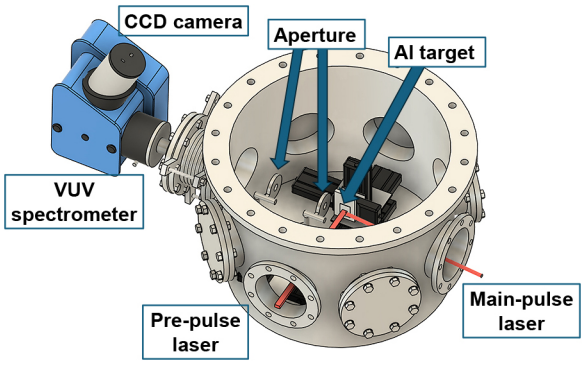

Fig. 4. A schematic diagram of the experimental setup for VUV emission measurement.

To measure the light emitted from the Al laser plasma, a normal incidence VUV spectrometer (Acton Research Corporation; VM-502, focal length 0.2 m, diffraction grating 1,200 grooves/mm) was used, with detection by a back-illuminated x-ray CCD (Princeton Instruments, PIXIS). The camera had 1,024 × 1,024 pixels with each size of 13 × 13 μm. Because the arrival time interval and energy of the two pulses were unstable from shot to shot due to some electric circuit problems, the measurements were accumulated over 30 shots. Wavelength calibration of the spectrometer at the central wavelength of 116.6 nm was performed using a mercury lamp and nitrogen plasma.

When both pulses were incident, intense scattering light of the main-pulse by the pre plasma and target surface in the direction of the spectrometer was observed. Therefore, apertures were placed near the target and in front of the spectrometer to block the scattered light from the main-pulse entering the spectrometer.

As described in Sec. 2, the pre-plasma was generated by irradiating the Al target with nanosecond pre-pulse, followed by the oblique incidence of a picosecond main-pulse to rapidly heat the low-density plasma region. The measurements were conducted by varying time delay between the two pulses, the incidence angle of the main-pulse, and the position of main-pulse irradiating on the plasma.

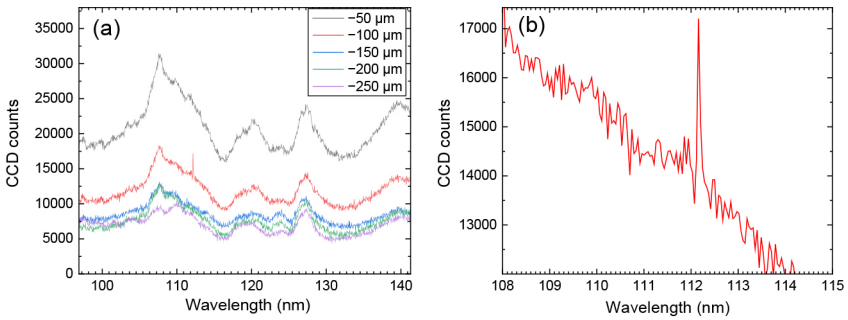

Fig. 5. (a) VUV spectra for various distance from target position (incident angle: 3.5°), and (b) narrow spectral spectrum corresponding to 111.9 nm lasing line.

4. Results and Discussion

Figure 5(a) shows the spectra for various laser irraidation positions from the target with a pulse arrival time difference of 5 ns and an irradiation angle of 3.5°. The red line represents the result when the main-pulse was irradiated onto the plasma located 100 μm from the target surface. Figure 5(b) show an enlarged view around 111-nm wavelength. A narrow spectral line appeared at 111.9 nm, which was not observed at other laser irradiation positions. This emission corresponds to the lasing transition of 111.9 nm spectrum of Al^{3+} ion of $3p$ ($^1S_0$)–$3s$ ($^1P_1$) transition and is observed as a relatively strong and isolated line, which may imply the presence of ASE phenomenon. However, definitive ASE characteristics —such as exponential intensity growth with plasma length, spectral narrowing, and reduction in beam divergence—have not been clearly confirmed yet. This is likely to be attributed to the narrow optimal window for ASE generation in terms of electron density and temperature. Furthermore, the instability of both pulse energies as well as their temporal jitter (up to 20 ns) hinders the observation of prominent ASE signal, likely resulting in the absence of strong emission.

5. Conclusion

In this study, an isolated 111.9 nm line emission from Ne-like Al ions was observed by means of the TCE and GRIP schemes (an incidence angle of 3.5°). While clear ASE signal has not been observed experimentally yet, the present study implies the potential for VUV ASE generation in Al laser plasmas. Strong emission of the sharp spectrum has not been obtained so far. The reason for this may be due to the narrow experimental conditions and plasma parameters required for the lasing action. Moreover, the fluctuations of the pre-pulse and main-pulse energies and the pulse arrival time interval could hinder the clear ASE measurement.

In the future, we plan to employ two dichroic mirrors (1,064 nm: transmitted, 112 nm: reflected) to block stray light entering the spectrometer, aiming to observe stronger ASE signals.

[1] K. Nagashima *et al.*, J. Plasma Fusion Res. **78**, 248 (2002).
[2] P.D. Baksh *et al.*, Sci. Adv. **6**, (2020).
[3] Y. Uehara *et al.*, Opt. Lett. **9**, 12 (1984).
[4] Y. Li *et al.*, Phys. Rev. A **52**, 4535 (1995).
[5] H. Daido and T. Kawachi, J. Plasma Fusion Res. **81**, 126 (2005).
[6] H. Daido *et al.*, Proc. SPIE **8849**, 884908 (2013).
[7] J.L.A. Chilla and J.J. Rocca, J. Opt. Soc. Am. B **13**, 2841 (1996).
[8] NIST Atomic Spectra Database, https://physics.nist.gov/PhysRefData/ASD/lines_form.html.
[9] Y. Li and J. Nilsen, Phys. Scr. **57**, 237 (1998).
[10] H.A. Sampson *et al.*, At. Data Nucl. Data Tables **53**, 23 (1993).
[11] J. Dunn *et al.*, Proc. SPIE **3156**, 102 (1997).
[12] A. Sunahara, J. Plasma Fusion Res. **89**, 416 (2013).